# COMBUSTION ANALYSIS OF MULTI-CIRCULAR JET PLATE IN INTERNAL MIXING AIR-ASSISTED ATOMIZER OF BURNER SYSTEM

**S.H. Amirnordin[1], A. Khalid[2,*], S. Sulaiman[2], D.W. Jacob[3], M. Fawzi[1] and S.M. Seri[2]**

[1]Centre for Energy and Industrial Environment Studies (CEIES),
Faculty of Mechanical and Manufacturing Engineering,
Universiti Tun Hussein Onn Malaysia, 86400 Parit Raja, Batu Pahat, Johor, Malaysia.

[2]Centre of Automotive and Powertrain Technology,
Faculty of Engineering Technology, Universiti Tun Hussein Onn Malaysia, 84600 Pagoh, Muar, Johor, Malaysia.

[3]Pusat Penelitian Advanced Creative Network, School of Electrical Engineering,
Telkom University, Terusan Buah Batu, 40257 Bandung, Indonesia.

*Corresponding Author's Email: amirk@uthm.edu.my

**Article History**: Received 10 December 2022; Revised 30 May 2023; Accepted 16 June 2023



**ABSTRACT:** Multi-Circular Jet (MCJ) plates have been identified as a turbulence generation system that can improve the performance of combustion. Most of the previous studies focused on the passive control method involve the changes in initial conditions of the systems including the geometry. However, the effects of primary air entrance of MCJ plates need to be investigated further. This paper aims to determine the effects of MCJ plates geometry on the burner combustion using the flame visualization technique. The plates are represented by P1, P2, and P3 characterized by the difference in the open area ratio at 17.8, 18.4 and 18.9 respectively. In the experiments, the flame images of all plates are captured at equivalence ratios of 0.8 to 1.2 using a Digital Single Lens Reflect camera. The flame temperatures are measured using the infra-red imaging technique while the emissions, burning chamber and stack temperature are also recorded using an emission gas analyzer and K-type thermocouples respectively. Image processing technique was used to analyze the data. Results show that an increase in open area ratio increases the flame temperature up to 11.4%. The result indicates that the open area ratio of

the MCJ plates is significant to the flame characteristics of the burner combustion.

**KEYWORDS:** *Air-assisted Atomizer; Burner; Combustion; Multi-circular Jet Plate; Open Area Ratio*

## 1.0 INTRODUCTION

Burners have been used as integral parts of boilers and industrial heating systems for the past centuries. In the burner system, atomizers are the most important component in mixing both the fuel and oxidizer. The atomizer transforms a certain volume of liquid into sprays or other types of dispersion into small drops to increase its surface area [1-3]. It discharges the liquid at high velocity into a relatively slow-moving stream of air or gases [4]. Another case in the air-assist atomizer is the form of external mixing, where high-velocity gas or steam is struck or collided on or outside the liquid of the discharge orifice. This type of mechanism has a better influence compared to the internal mixing as it prevents back pressure due to the communication between gas and liquid [4-7]. Contrary to that, it seems to be less efficient compared to the internal-mixing method as higher flow rates of gaseous are needed to obtain a similar degree of atomization. The articles present both internal and external mixing advantages and disadvantages. However, further works are needed to investigate in more detail the effects of the flame.

The performance of an air-assisted atomizer depends on its size, geometry and physical properties of the dispersed phase (liquid), and continuous phase (pressurized air). It is designed to improve the fuel-air mixing before spraying. It has advantages due to the high control for various and broad applications, which has been studied intensively by many researchers [5-8]. Instead, it also has advantages including good spray quality at low pressure, easy-to-control spray performance, and low primary air consumption compared to the external mixing of air-assisted atomizers [9]. The atomizer nozzle geometry plays an important role in the characteristics of spray atomization [10] and mixture formation of fuel-air, which contribute in enhancing the combustion and reducing the emissions [11]. Many factors influence the spray performance including the gas-to-liquid ratio, air and liquid injection pressure [12,13], liquid properties [14], and geometry of atomizers [10,15]. The previous studies [10,16-18] have been focused on the effects of geometrical parameters on the spray formation and the interaction characteristic of fuel and air in a mixing chamber. The result

shows that the diameter of the air channel and liquid ports have played a major role in influencing the SMD. A decrease in air injection area and injection length also can reduce the droplet size of a spray [10].

Previous research reported on the performance of the atomizers based on the geometries and physical properties. However, further investigation is required to analyze the impacts of open areas on flame combustion. This paper intends to investigate the geometrical configurations of the MCJ plate especially on the entrance open area and its relation to the fuel-air mixing. These parameters are studied in order to obtain the dependence of the atomizer's characteristics on the air-fuel mixing ratio (equivalence ratio) and geometrical of the plate. It is anticipated that this approach has a high potential for improving the fuel and air mixing in the atomizers and, hence can assist in controlling the combustion of the burner.

## 2.0 METHODOLOGY

Testing facilities were set up using the spray chamber and burning chamber. The atomizer was placed vertically in the galvanized iron chamber 200 cm by 200 cm cross-section and 170 cm height. The height of the chamber was 130 cm from the floor while the exhaust ducting was 110 cm height from the top of the chamber. One of the walls was fitted with the 15 cm × 15 cm with 1 cm thickness of tempered glass for visual access inside the chamber. A special access for maintenance purposes was built at the side of the wall to ignite the burner. The top of the chamber was connected to a blower which directly connected to the environment outside the laboratory which will create atmospheric pressure of the chamber outlet. The bottom of the chamber was equipped with the excess fuel trap system.

Table 1 shows the diesel properties used in this experiment. The air-assisted atomizer has been fabricated based on the previous work [10, 19] except for the MCJ plates. Figure 1 shows a schematic diagram of the experimental setup. It is equipped with an air compressor unit, an electric fuel pump, a blower for secondary air, a combustion chamber, and an atomizer unit. The air (primary air) for the atomizer is supplied from the compressor. The secondary air is delivered from a blower right to the bottom of the injector by using an 8 cm diameter of the piping. The primary air mass flow rate is controlled by the valve on the pressure gauge and continues to be channeled to the atomizer. The diesel fuel flow rate is controlled by the voltage regulator and connected to the mass flow meter to ensure the correct reading for each experiment. The enlarged diagram shows the detail section of the

atomizer. There is a mixing chamber in which the mixing of fuel and air occurs before being sprayed for atomization. The nozzles consist of eight holes with 1 mm diameter. This atomizer uses fuel (diesel) and air supplied by the system. The atomizer is equipped with an air compressor connected to the vertical compressed air stabilizer to supply the primary air at 0.1 MPa (1 bar) as shown in Table 2. The calculation is performed to determine a suitable amount of fuel and air considered in the equivalence ratio (Table 3).

Three MCJ plates are considered in this study. This plate delivers the fuel and air, which is originally from different channels to the mixing chamber. The chamber functions to mix air and fuel before discharging the mixture. The effects of geometrical MCJ plates are studied by characterizing atomizers according to their geometry. Plates P1, P2, and P3 are selected due to their variations in terms of open area ratio as depicted in Figure 2 and Table 4. The values of the open area ratio increase from 17.8, 18.4 and 18.9 for P1, P2 and P3 respectively. In this study, the presence of circular holes functions as turbulence generators to boost the turbulence levels and improve the mixing of fuel and air. The open area ratio is obtained by dividing the open area to the blockage area of the plate. The open area ratio determines the amount of air entering the mixing chamber.

The equivalence ratio (ER) is defined as the air-fuel ratio of complete combustion divided by the actual air-fuel ratio. For stoichiometric reaction, ER is equal to 1, the quantity of oxidizer is sufficient to burn fuel and produce complete products of combustion. If the quantity of oxidizer exceeds the stoichiometric proportion, it is called lean mixture, where ER is less than 1. If the quantity of oxidizer is less than the stoichiometric, where ER is more than 1, it is called rich mixture. For lean mixtures (0.8 and 0.9), it is more efficient compared to rich mixtures (1.1 and 1.2). This is less efficient combustion, but it produces more power and higher emissions. The ER is varied by changing the amount of fuel supplied to the mixing chamber from 4.94 kg/hr to 7.41 kg/hr.

Table 1: Properties of turbo diesel Euro 5 [20]

| Property | Unit | Value |
|---|---|---|
| Relative density at 15° C | kg/l | 0.84 |
| Flash point | °C | 60 |
| Viscosity at 40°C | cST | 2.0-4.5 cSt at 40°C |

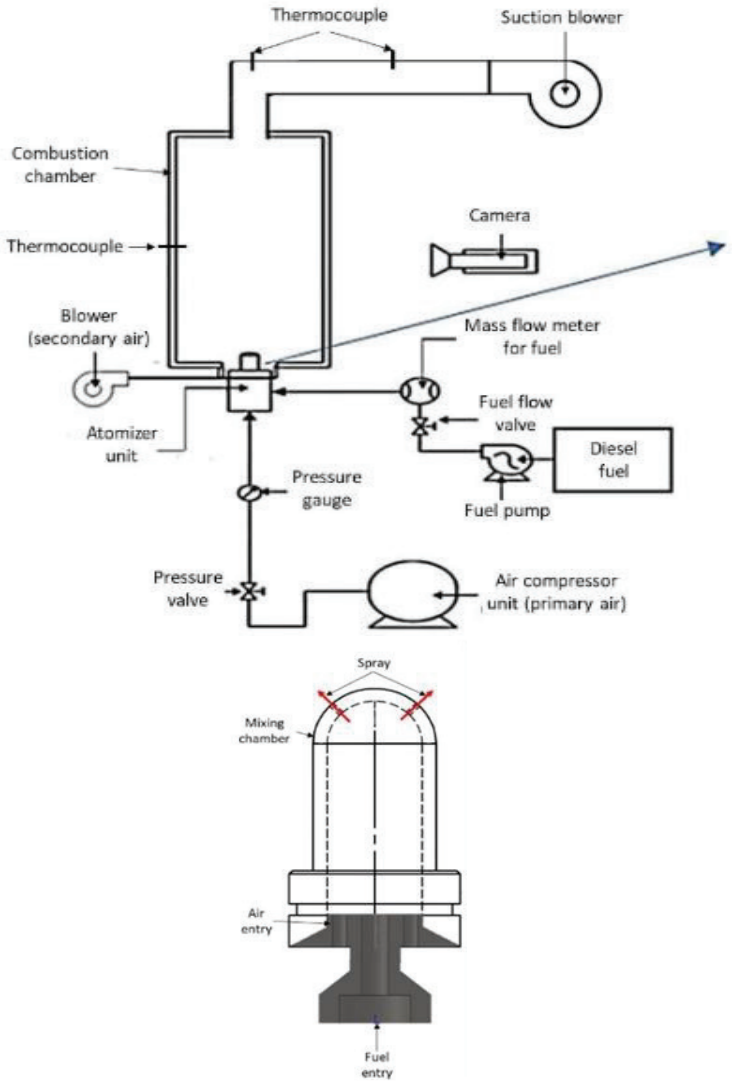


Figure 1: Schematic diagram of the experimental setup

Table 2: Equipment specifications

| Measuring point | Equipment | Model no. | Measuring range |
|---|---|---|---|
| Fuel inlet | Mass flow meter | Ono Sokki FZ-2100 | 0.2 – 82 kg/h |
| Primary air inlet | Airflow meter | Dwyer RMA-33-SSV | 0 – 120 cc/min |
| Secondary air inlet | Pitot tube with a digital micro manometer | Dwyer series 160-8 | 0-100 Pa |

Table 3: Operating conditions

| Plate | Air pressure, bar | Air density at 30°C, kg/m³ | Ambient temperature, K | Fuel mass flow rate, kg/hr |
|---|---|---|---|---|
| 1,2,3 | 1.0 | 1.184 | 300 | 4.941 - 7.412 |

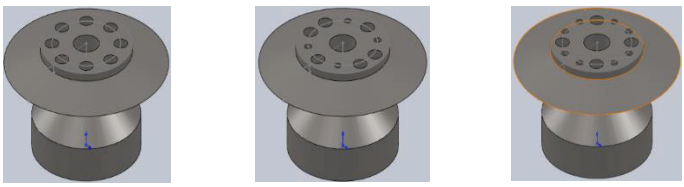

(a) (b) (c)

Figure 2: Geometries of the plate; (a) P1, (b) P2 and (c) P3

Table 4: Specification of the plates

| Plate 1 | Plate 2 | Plate 3 |
|---|---|---|
| Diameter 2 mm × 8 holes; Open area ratio, Ae =17.8 | Diameter 2 mm × 6 holes; Diameter 1.5 mm × 4 holes; Open area ratio, Ae =18.4 | Diameter 2 mm × 4 holes; Diameter 1.5 mm × 8 holes; Open area ratio, Ae =18.9 |

The flame images are recorded using a DSLR Nikon D90 (without lighting) with a 1/4000 s camera shutter speed. The lens is focused perpendicular to the nozzle for obtaining the full image of the flame. A single 10 cm bar is located next to the nozzle as a calibration length for pixel. The recording has been lasted for 2 minutes from the ignition of the flame until the extinguished flame due to high safety precautions during the experiment. Video of the recorded flame has been loaded to software for converting to still images. The 10 images are selected to represent stable and consistent flame. These images are taken at arbitrary time intervals between images. These images has been anayzed further using image processing software, ImageJ. The measuring tools are required to be calibrated first with the 10 cm bar besides the flame. By adjusting the threshold values for automatic adjustment, the images are analyzed, then flame angle and flame height are measured as shown in Figure 3 (a) and (b). The flame angle is measured from the maximum boundary of flame to the horizontal plane of the burner. The flame height is determined by measuring the distance from the top of the burner to the farthest point of the flame. For all the collected results, the mean values and standard deviation are calculated to determine the acceptable results of the measurement. The percentage of increment or decrement can be determined by the calculation using

$$\left[\frac{new\,number - original\,number}{original\,number}\right] \times 100 \quad (1)$$

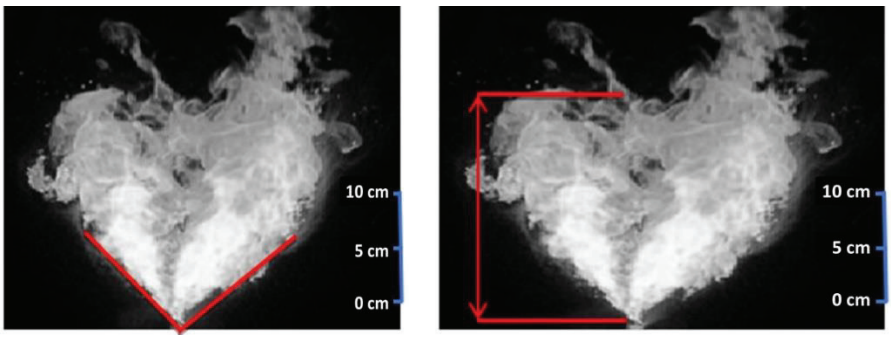


(a) (b)

Figure 3: Flame images showing: (a) flame angle; (b) flame height

High temperature flame and highly turbulence flame might cause typical K-type thermocouple not suitable to detect the temperature. Thus, the flame temperature profile can be determined by using the infrared camera and thermal analysis software. The camera has special sensor technology to convert heat emitted by the flame into color images. These color images allow the observation in temperature differences being read as a fraction of degrees. In this study, thermal camera model FLIR 640 is used for thermal image recording, while FLIR Quick Report is used as the analysis and reporting software. The verification of the IR camera is conducted by measuring the temperature of one point of the flame using a thermocouple. Once this point temperature is known, the temperature is also measured by the IR camera. During this period, the emissivity value setting on the IR camera must be modified until the temperature obtained by the IR camera and the thermocouple coincides.

Global emissions are measured by using a sample probe, which is inserted at the top of the chimney. The Autocheck Gas & Smoke Gas Analyzer is used with the flue measuring probe. It is equipped with $O_2$ sensor and use non-dispersive infrared measurement to measure HC, CO and $CO_2$; while $O_2$ and $NO_x$ use electro chemical cell. The warm-up time is normaly less than 20 seconds. However, the response time is less than 8 seconds for HC, CO and $CO_2$ while the response time is less than 10 seconds for $O_2$ and $NO_x$. However, in this paper only the emissions from the HC and CO are analyzed and discussed.

## 3.0 RESULTS AND DISCUSSION

Combustion of liquid fuel can only be accomplished if the liquid is converted into droplets known as a spray. Atomizers are designed to disintegrate this liquid fuel into the spray of droplets. This increases the fuel surface, thus enhances the combustion rate due to an increase in evaporation rate. In the air-assisted atomizers, the primary air and fuel spray produce highly enough momentum to dominate the combustion. This section discusses the results of flame angle and flame height related to the fuel and air mixing, which are influenced by the geometrical configurations of the MCJ plates. In this system, the characteristics differ from the premixed flame and the diffusion flame since the composition of droplets is not uniform. The droplets vary in sizes, move in various direction at different velocities into the air mainstream. Lack of uniformity in this unburnt mixture produces irregularities which affect the flame propagation, hence giving the non-uniform shape of the flame . The characteristics of this type of flame can be related to droplet diffusion flames which gives the yellow color of the flame.

### 3.1 Flame Analysis

The experiments are conducted for all ER. Figure 4 shows the processed images of flame for P1, P2 and P3 produced from the burner. Each of this ER represents the lean, stoichiometric and rich mixtures. The results obtained is sufficient to show the resulting flame influenced by the ratio of fuel and air in the burner system.The combustion was found to occur at rich mixtures only. It is shown that each plate produces its own flame characteristics, thus provides its own shape. However, it also depends on the ER, which is influenced by the fuel and air mixing rate into the mixing chamber.

Generally, combustion is formed when air and diesel fuel are mixed. However, it produces different flame angle and flame height, depending on the mixing condition. Figures 5(a) and 5(b) show the flame angle and flame height for a different ER. It is observed that the P1, P2, and P3 only produce combustion at rich mixture. Figure 5(a) shows the flame angle varies from 87.1° to 97.5° as the ER increases. Calculations show that an increment up to 11% of the flame angle is seen for these plates. Figure 5(b) shows the changes in the flame height for different ER. An increase in ER has a significant impact on the flame height for P3 only. It causes an increment up to 10.8% for P3. However, for plates P1 and P2; the different in flame height is not so significant. It is noted that P3 with the highest open area exhibits the largest flame angle and the highest flame height of 97.5° and 191.9 mm, respectively.

For both cases, ER is essential in influencing the flame angle and flame height for the combustion from the air-assisted atomizer.

(a) (b) (c)

Figure 4: Flame images: (a) P1, (b) P2 and (c) P3 at ER 1.2

Trend shows P1 does not produce combustion from lean to stoichiometric mixtures. As the open area ratio increases for P2 and P3, the combustion is still not occurred. Nevertheless, higher ER which indicates higher fuel flow rate increases the mixing rate, hence increases the kinetic energy of fuel and air. That is the reason the combustion occurs at rich mixtures. It improves the mixing of fuel and air rate due to the presence of stronger flow recirculation, hence produces stable combustion.

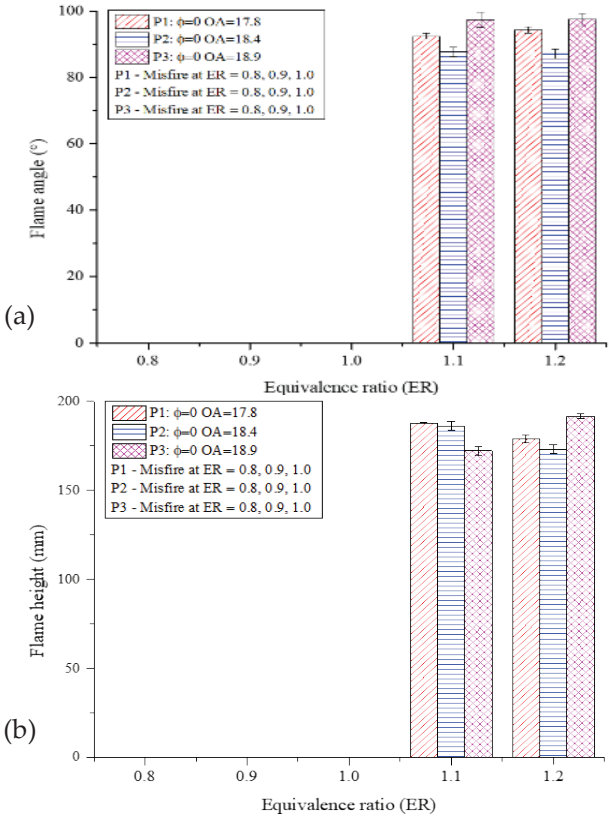


Figure 5: (a)Flame angle and (b) flame height of the multi-hole nozzle for P1, P2, and P3

### 3.2 Flame Temperature Analysis

This section involves the temperature analysis of flame. Infrared thermography is used as a part of non-intrusive technique on the flame temperature, which can be calculated from the change of physical parameters. The colors represent the flame temperature of all objects within the frame. The white color represents the highest temperature at 447.5 ˚C, which is located at the most inner side of the flame. The temperature decreases outside of the flame with the purple color shows the lowest temperature at 51.8 ˚C. In this section, the main data is the highest flame temperature achieved at certain conditions.

Figure 6 (a) and (b) shows the thermal images of flames with the influence of MCJ plates under different ER. The parameter of primary air that kept constant is pressure at 0.1 MPa (1 bar). This corresponds to fuel density of $\varrho$ = 0.8337 kg/m$^3$. At higher ER, the thermal image becomes larger due to an increase in the amount of fuel and air mixture. An increase in the temperature is also recorded. Results show that at low ER, the misfire occurs for P1, P2, and P3. The combustion occurs only at high ER. It is noted that the temperature increases with an increase in the ER.

In Figure 7, the maximum temperature is obtained for P1, which the temperature increases from 574 ˚C to 622 ˚C (an increment of 8.4%). A similar trend is also seen for P2 and P3, which show a temperature increment of 9% and 5% respectively. The relatively large percentage difference is seen due to the combustion is only occurred at high ER for P1, P2, and P3. Furthermore, the effects of the open area ratio are also examined here. For ER 1.2, the flame temperature decreases from 622 ˚C to 551 ˚C, represents a decrease of 11.4%, as the open area increases from 17.8 to 18.9. A similar trend also occurs for ER 1.1; the temperature exhibits 8.5% decreases. It is inferred that the open area ratio of the MCJ plates influenced the flame temperature. This is due to the changes in fuel and air supply to the combustion area.

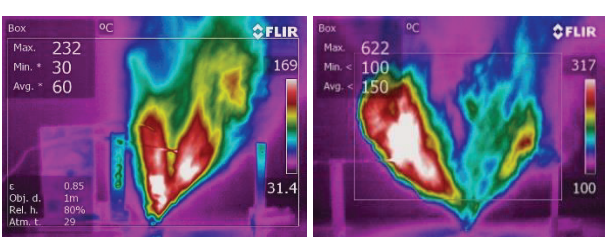


(a) (b)

Figure 6: Thermal images of flame from P1 at (a) ER=1.1 and (b) ER=1.2

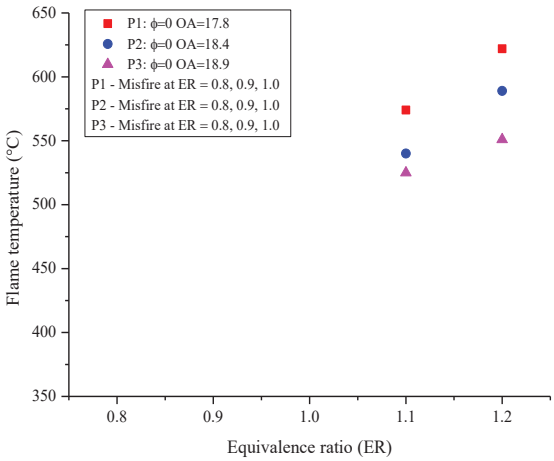


Figure 7: Flame temperature of the multi-hole nozzle for P1, P2, and P3

### 3.3 Emission Analysis

This section discusses the geometrical effects of the plate on the emissions from the combustion. In this paper, CO and HC concentration are presented at different open area. Figure 8(a) shows the effect of the ER and the open area ratio on the emission concentration of CO. It is observed that there is no combustion (misfire) occurs for P1, P2, and P3 plates for the ER from 0.8 to 1.0. Therefore, in this section, the measurements for these plates are taken for the ER only from 1.1 to 1.2. It shows that CO emission is increased 34.5% for P1 as the ER increases from 1.1 to 1.2. However, CO emission decreases for P2 and P3 about 8.7% and 46.7%, respectively. For P2 and P3, by increasing the air-fuel ratio (as the ER increases), the flame temperature increases, thus produces lower CO levels. However, P1 has shown the reverse effect where the CO emission increases as the ER increases.

Another aspect of the analysis is an increase in the open area of plates for primary air entering the mixing chamber between P1, P2, and P3 has increased the CO emission up to 47.2%. An increase in the open area reduces the volume flow rate of air entering the chamber; hence reduces the mixing intensity, reduces the flame temperature and finally has increased the CO levels. The results presented here are also in agreement with the work by [6]. Although the flame temperature increases but the value of temperature is still below the 1000 K, so that it can increase the CO emission for different cases. Figure 8(b) shows an almost identical trend is also found for HC emission. It is noted that, an increment in the ER increases the emission of P1 and P3 to 2.6% and 4.8% respectively. However, for high ER, an increase in the open area

ratio manages to reduce the emission of P1 and P3 at 45.3% and 58.4%, respectively. This is desired in burner combustion as the more complete combustion can reduce the HC.

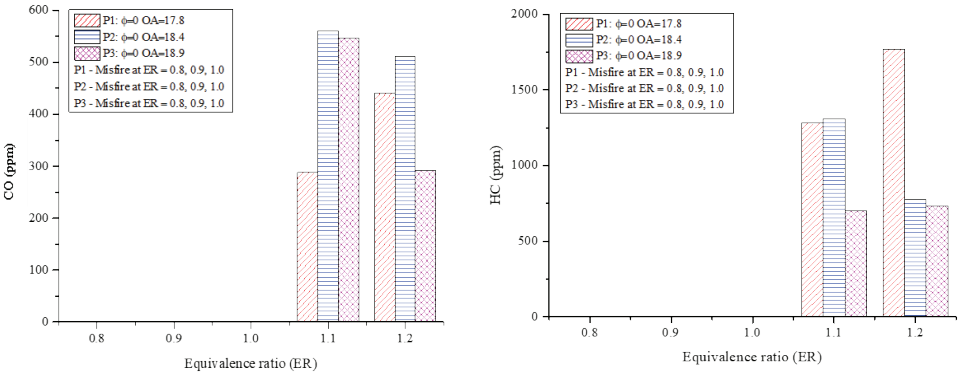


Figure 8: Emission of: (a) CO and (b) HC for P1, P2, and P3

## 4.0 CONCLUSION

The open area ratio of the jet hole of the atomizer air inlet has significant influence on atomization in the atomizer. Results show that the open area ratio at 17.8, 18.4, and 18.9 influence the atomization and finally affects the flame characteristics and the emissions concentration, Besides, the air and fuel ratio (represented by ER) also plays an important role in the combustion of this system. The open area ratio of the MCJ plates has shown its effectiveness to determine the combustion characteristics from the burner.

## ACKNOWLEDGEMENTS

The authors would like to thank the Ministry of Education Malaysia for supporting this research under the Fundamental Research Grant Scheme No. FRGS/1/2019/TK10/UTHM/02/7 Vot K218, GPPS U749 and partially sponsored by Universiti Tun Hussein Onn Malaysia.

## AUTHOR CONTRIBUTIONS

S.H. Amirnordin: Experimental, Data Measurements, Writing-Original Draft Preparation; A. Khalid: Flame Image Capturing, Image Analysis, Supervision; S. Sulaiman: Conceived, Designed the Data Analysis; D.W. Jacob: Analysis, Results Interpretation; M. Fawzi:

Study Conception, Design, Samples Characterized; S. M. Seri: Methodology, Performed the Experiments, Writing-Reviewing and Editing.

## CONFLICTS OF INTEREST

The manuscript has not been published elsewhere and is not under consideration by other journals. All authors have approved the review, agree with its submission and declare no conflict of interest on the manuscript.

## REFERENCES

[1] A. Khalid, M. Suardi, R.Y.S. Chin and S.H. Amirnordin, "Effect of biodiesel-water-air derived from biodiesel crude palm oil using premix injector and mixture formation in burner combustion", *Energy Procedia*, vol. 111, pp. 877-884, 2017.

[2] A. Khalid, S.H. Amirnordin, U. Vasuthavan, A. Hariri and M. Fawzi, "Spray formation in the multi-hole nozzle of twin-fluid atomizers", *Journal of Advanced Research in Fluid Mechanics and Thermal Sciences*, vol. 53, no. 1, pp. 75-81, 2019.

[3] S.H. Amirnordin, A. Khalid, M. Suardi, B. Manshoor and M.F. Hushim, "Effects of fractal grid on spray characteristics and flame development in burner combustion," in the *15th Asian Congress of Fluid Mechanics*, Kuching, Sarawak, 2016, pp. 1-5.

[4] M. Fawzi, and K. Yoshiyuki, "Natural gas combustion inside a confined volume chamber using gas-jet ignition method", *Journal of Advanced Manufacturing Technology*, vol. 8, no. 2, pp. 1-12, 2014.

[5] Y. M. Arifin, M. Z. Mokhtar, M. Z. Akop, S. A. Shamsudin, F. Syahrial, and S. G. Herawan, "The effect of diesel and bio-diesel fuel deposit layers on heat transfer", *Journal of Advanced Manufacturing Technology,* vol. 13, no. 2, pp. 1-14, 2019.

[6] A. M. Najib, and D. Waechter, "Swirl fluid flow nozzle: A solution for fluid jet polishing process", *Journal of Advanced Manufacturing Technology*, vol. 15, no. 1, pp. 15-26, 2021.

[7] A. A. A. Asady, and H. H. S. Alhafid, "Theoretical and experimental study of jet vectoring in subsonic flow for circular nozzle", *Journal of Advanced Manufacturing Technology*, vol.9, no. 2, pp. 1-12, 2015.

[8] A. Mashayek and N. Ashgriz, *Handbook of Atomization and Sprays: Theory and Applications*, New York: Springer Science & Business Media, 2011.

[9] F. Liu, A.E. Karataş, Ö.L. Gülde, and M. Gu, "Numerical and experimental study of the influence of $CO_2$ and $N_2$ dilution on soot formation in laminar coflow $C_2H_4$/air diffusion flames at pressures between 5 and 20 atm", *Combustion and Flame*, vol. 162, no. 5, pp. 2231-2247, 2015.

[10] J.A. García, A. Lozano, J. Alconchel, E. Calvo, F. Barreras and J. L. Santolaya, "Atomization of glycerin with a twin-fluid swirl nozzle", *International Journal of Multiphase Flow*, vol. 92, pp. 150-160, 2017.

[11] M. Zaremba, L. Weiß, M. Malý, M. Wensing, J. Jedelský and M. Jícha, "Low-pressure twin-fluid atomization: Effect of mixing process on spray formation", *International Journal of Multiphase Flow*, vol. 89, pp. 277-289, 2017.

[12] A. Williams, *Combustion of Liquid Fuel Sprays*. Oxford: Butterworth-Heinemann, 2013.

[13] T. Yatsufusa, Y. Kidoguchi and D. Nakagawa, "Improvement of emissions and burning limits in burner combustion using an injector on the concept of fuel-water internally rapid mixing", *Journal of Energy and Power Engineering*, vol. 8, no. 1, pp. 11-17, 2011.

[14] A. Kushari, "Effect of injector geometry on the performance of an internally mixed liquid atomizer", *Fuel Processing Technology*, vol. 91, no. 11, pp. 1650-1654, 2010.

[15] T. Yatsufusa, T. Kumura, Y. Nakagawa, and Y. Kidoguchi, "Advantage of using water-emulsified fuel on combustion and emission characteristics", *Fuel,* vol. 5, no. 60, 2009.

[16] J. Barroso, A. Lozano, F. Barreras, and E. Lincheta, "Analysis and prediction of the spray produced by an internal mixing chamber twin-fluid nozzle", *Fuel Processing Technology*, vol. 128, pp. 1-9, 2014.

[17] Z. Li, Y. Wu, H. Yang, C. Cai, H. Zhang, K. Hashiguchi, and J. Lu, "Effect of liquid viscosity on atomization in an internal-mixing twin-fluid atomizer", *Fuel*, vol. 103, pp. 486-494, 2013.

[18] G. Ferreira, J. A. García, F. Barreras, A. Lozano, and E. Lincheta, "Design optimization of twin-fluid atomizers with an internal mixing chamber for heavy fuel oils", *Fuel Processing Technology*, vol. 90, no. 2, pp. 270-278, 2009.

[19] S. H. Yoon, D. K. Kim, and B. H. Kim, "Effect of nozzle geometry for swirl type twin-fluid water mist nozzle on the spray characteristic", *Journal of Mechanical Science and Technology*, vol. 25, pp. 1761-1766, 2011.

[20] J. A. García, A. Lozano, J. Alconchel, E. Calvo, F. Barreras, and J. L. Santolaya, "Atomization of glycerin with a twin-fluid swirl nozzle", *International Journal of Multiphase Flow*, vol. 92, pp. 150-160, 2017.

[21] S. Lal, A. Kushari, M. Gupta, J. C. Kapoor, and S. Maji, "Experimental study of an air assisted mist generator", *Experimental Thermal and Fluid Science*, vol. 34, no. 8, pp. 1029-1035, 2010.

[22] S. G. Daviault, O. B. Ramadan, E. A. Matida, P. M. Hughes, and R. Hughes, "Atomization performance of petroleum coke and coal water slurries from a twin fluid atomizer", *Fuel*, vol. 98, pp. 183-193, 2012.

[23] D. Das, V. Pathak, A. S. Yadav, and R. Upadhyaya, "Evaluation of performance, emission and combustion characteristics of diesel engine fueled with castor biodiesel", *Biofuels*, vol. 8, no. 2, pp. 225-233, 2017.